Supporting Information

Schneider et al. 10.1073/pnas.1121252109

SI Methods

Fly Stocks. *Canton-S* and *Oregon-R* wild-type flies were obtained from J. C. Hall (Emeritus at Brandeis University, Waltham, MA). Auditory-impaired iav^1 flies were from the Bloomington stock center (#6029). w^{1118}, and w^{1118};;$Orco^2$ [née $Or83b^2$ (1)] were obtained from L. Vosshall (The Rockefeller University, New York, NY). The taste-deficient mutant (w $\Delta XBs6$; $Poxn^{\Delta M22\text{-}B5}$) and its control ($w$; $Poxn^{\Delta M22\text{-}B5}$ $Super^{A\text{-}207\text{-}2}$) were obtained from M. Noll (University of Zurich, Zurich, Switzerland). $Orco^2$ was established in a *Canton-S* background and compared with a w^{1118} background. Only the statistical differences that repeated in both backgrounds were reported.

Treatments. Female flies were collected within 4 h of eclosion, ensuring virginity, and males were collected within 12 h of eclosion. All collections were under light anesthesia (CO_2) and grouped by genotype and sex into vials. Each vial contained 12–16 flies (except for isolated; Fig. S5) and were kept at 12 h light/12 h dark for 3 d and at 25 °C before use in an experiment. Fifteen minutes before the start of an experiment, flies were gently mouth-pipetted into the semiopaque Plexiglas arena (60-mm diameter × 2-mm height) covered with transparent Plexiglas. The arenas were undisturbed for at least 10 min before the start of acquisition. For *Canton-S* males in the dark, the lights turned off 10 min before the start of the experiment (to avoid the startle response during acquisition)—thus total time between setup and recording was equal in all treatments. For all groups, the arenas were back illuminated by far-red lighting (DealExtreme part no. 15235).

Digital video was captured by a FireflyMV (Point Gray) firewire camera using fview (2). Thirty minutes of video was analyzed using Ctrax (3) to obtain fly orientation, position, and trajectories. Scripts were written in MATLAB to import tracked data and identify when an interaction occurred between specific flies, defined by rules outlined in Fig. 1*A* (minimum distance, required orientation, and maintenance of these for a specified time frame). A subsample of trials was taken, and interaction sequences were exported using MATLAB scripts and MEncoder to be manually scored.

Iterative Network Analysis. The interactions throughout a trial were flagged, and a connectivity matrix (CM_1) was used to accumulate the critical number of unique interactions and stored. The second connectivity matrix (CM_2) was constructed by ignoring the first interaction and accumulating the subsequent critical amount of unique interactions. The ith connectivity matrix (CM_i) ignored the first $i - 1$ interactions. This continued until there were insufficient interactions left to fill a connectivity matrix, with at most critical value − 1 unique interactions left nonanalyzed (8.2% of total interactions in wild-type strains for 25% density). Although weighted connection matrices were produced, all subsequent analyses were carried out on unweighted (binary) connectivity matrices. Brain Connectivity Toolbox (4) MATLAB scripts were used for network measurements and motif identification. Each network measurement was calculated for every network within the trial, and these were averaged for subsequent analysis.

Generation of Artificial Networks. For each treatment group, artificial networks were constructed by selecting 12 trials at random from those within the treatment that displayed at least 33 unique interactions. From each of those 12 trials, one fly was chosen at random, and their entire trajectories were normalized in space (to compensate for any image distortion during acquisition relating to cameras/lenses) and combined (Fig. S1). Artificial networks were constructed by evaluating the combined trajectories for interactions according to the same criteria of orientation and distance (Fig. 1*A*); however, the time criterion was lowered to 0.01 s (owing to the artifact of flies being able to occupy and pass through the same pseudospace without stopping). Each artificial network was limited to generating a set number of networks, this being determined by the median number of networks their treatment group generated.

Statistical Analyses. ***Randomness tests.*** Because all our networks have 12 flies and 33 interactions, we used the variance of the degrees to compare degree distributions. Within each trial, for each network iteration, we calculated the variance of the degrees. We compared the mean variance for each trial against both the median of the variance of the degree distribution of 10,000 Erdős–Rényi graphs and the median of the mean variance of the degree distribution of 1,000 of their respective artificial networks; for wild-type genotypes and strains, for mutants and controls, 500 artificial networks were generated. We used a sign test to test whether the proportion of networks having a higher variance was significantly different from the null hypothesis (50%).

Preferential attachment. Each network within the trial was analyzed; the degree of a fly was determined when the network was five interactions short of completion. The subsequent five incoming interactions were then recorded against the receiving fly's degree, and the normalized probability was calculated and plotted. Each trial generated at most one data point for each degree, which was calculated as the mean of the probability of receiving an incoming interaction for that degree.

Fly behavior measurements. Movement, average time spent per interaction, interaction rate, and percentage of interactions reciprocated were analyzed with either two-factor ANOVAs (strain and sex) or one-factor ANOVAs. Because of nonnormality and unequal sample size, each test's F statistic (including factor and interaction) were compared with an empirical distribution, this was accomplished by permuting the group identity in each test 10,000 times and establishing a distribution of the statistic under the null hypothesis (5). To correct for multiple testing, the false discovery rate was controlled between the behavioral measurements (6).

Structural measurements. All trials were standardized to control for the degree distribution. For each iteration, 10,000 random networks were generated with the same in- and out-degree distributions (for 25% density, for all other densities, 500 random networks were generated). Each measurement was calculated for the observed as well as every generated to generate a z score (used for all statistical analyses of network properties):

$$(\text{measurement}_{\text{observed}} - \text{mean}(\text{measurement}_{\text{random}}))/\text{std}(\text{measurement}_{\text{random}}).$$

Univariate analysis permutations and multiple test correction were carried out as above. To correct for multiple testing, the false discovery rate was controlled between the four network measurements. Fig. S7 shows analysis of triadic interactions [motifs (7)] and discriminant analysis classifiers.

1. Larsson MC, et al. (2004) Or83b encodes a broadly expressed odorant receptor essential for Drosophila olfaction. *Neuron* 43:703–714.
2. Straw AD, Dickinson MH (2009) Motmot, an open-source toolkit for realtime video acquisition and analysis. *Source Code Biol Med* 4:5.
3. Branson K, Robie AA, Bender J, Perona P, Dickinson MH (2009) High-throughput ethomics in large groups of Drosophila. *Nat Methods* 6:451–457.
4. Rubinov M, Sporns O (2010) Complex network measures of brain connectivity: Uses and interpretations. *NeuroImage* 52:1059–1069.
5. Manly BFJ (2007) *Randomization, Bootstrap and Monte Carlo Methods in Biology* (Chapman & Hall/CRC, Boca Raton, FL).
6. Benjamini Y, Hochberg Y (1995) Controlling the false discovery rate: A practical and powerful approach to multiple testing. *J R Stat Soc Ser B* (*Methodological*) 57: 289–300.
7. Milo R, et al. (2002) Network motifs: Simple building blocks of complex networks. *Science* 298:824–827.

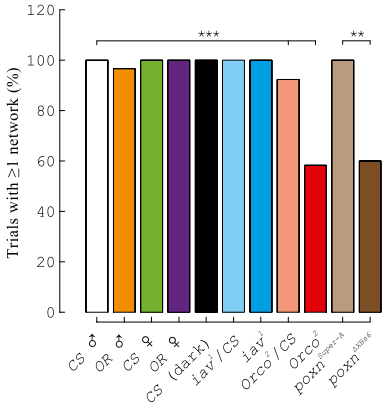

Fig. S1. Ability to form social interaction networks in wild-type and mutant flies. Proportions of trials that resulted in at least one network of 25% density are plotted. Both *Orco*^{2} and *poxn*$^{\Delta XBs6}$ had significant reductions in number of trials resulting in at least one network (*Canton-S* vs. *Orco*^{2}/*Canton-S* vs. *Orco*^{2} Fisher's exact $P < 0.001$; *poxn*$^{Super\text{-}A}$ vs. *poxn*$^{\Delta XBs6}$ Fisher's exact $P < 0.001$). *$P < 0.05$, **$P < 0.01$, ***$P < 0.001$, if significance is maintained after multiple test corrections. Significant effects of *Orco*^{2} were observed in both a *Canton-S* as well as a w^{1118} background [w^{1118} (n = 24/25), (w^{1118})Orco2/w^{1118} (n = 21/24), (w^{1118}) Orco2 (n = 13/26)].

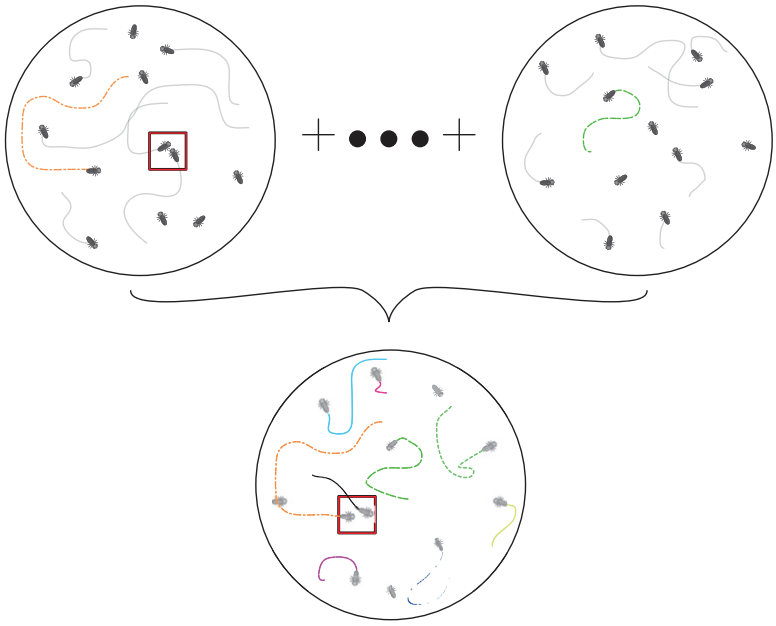

Fig. S2. Generation of virtual networks. For each treatment, 12 trials were selected at random from those that displayed a successful network. From each of those 12, one fly was chosen at random, and their entire trajectories were combined into one artificial network. These artificial networks were then evaluated for interactions according to the same criteria of orientation and distance. However, there was no criterion for time, owing to the artifact of two flies being able to occupy and pass through the same virtual space. Interactions are identified with boxes.

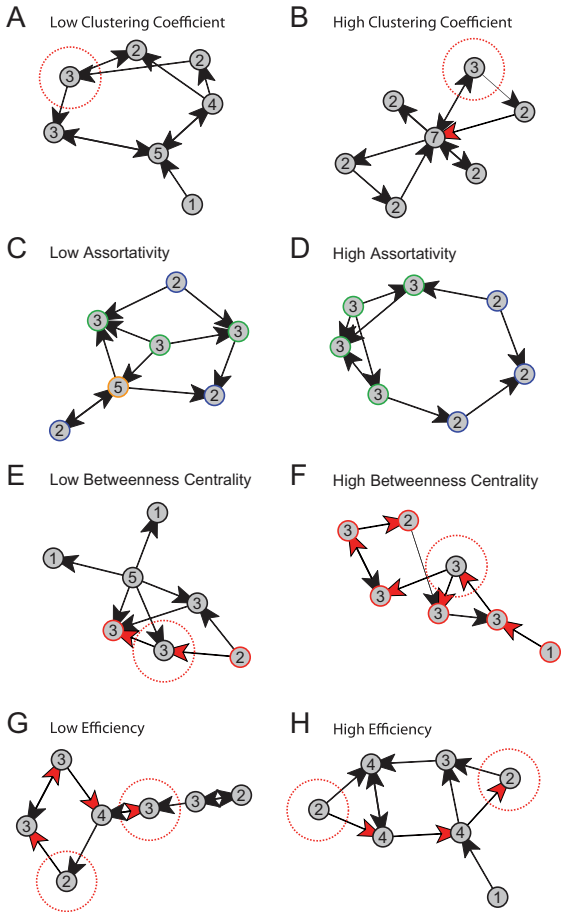

Fig. S3. Visualization of network measurements. (*A* and *B*) Clustering coefficient reflects the interconnectedness of the nodes (individuals) in a given network. Example nodes (dotted red circles) demonstrate that in networks with low clustering coefficients (*A*), neighbors are unlikely to interact, whereas in networks with a high clustering coefficient (*B*), neighbors are more likely to interact (red arrow indicating interaction between neighbors of example node). (*C* and *D*) Assortativity is the correlation between nodes of similar degree. Low assortativity (*C*) indicates a tendency of nodes of dissimilar degree to interact, whereas high assortativity (*D*) indicates a positive correlation between nodes of like degree. Nodes are color-coded for degree to visualize the tendency of like nodes interacting. (*E* and *F*) Betweeness centrality is a measure of how many shortest paths traverse a node, which can indicate the relative importance of a node for information flow. In the example network with low betweeness centrality (*E*), very little information relay happens; the node exhibiting the highest amount of relay (dotted red circle) only acts as an intermediary between two nodes (red nodes; information relay indicated with red arrows). In the example network with high betweeness centrality (*F*), some nodes (e.g., dotted red circle) relay information between many other individuals in the network (red nodes; information relay indicated with red arrows). (*G* and *H*) Efficiency of a network is a measurement of the average shortest path length that information would flow through. Lower efficiency score (*G*) indicates less efficient information flow on average. Information relay throughout the network takes relatively more steps between nodes (dotted red circles, four-step information relay indicated with red arrows). A network with a relatively higher score (*H*) is generally evenly distributed and has much lower steps between nodes (dotted red circles, three-step information relay indicated with red arrows). In *A*–*F*, degrees are indicated in the nodes.

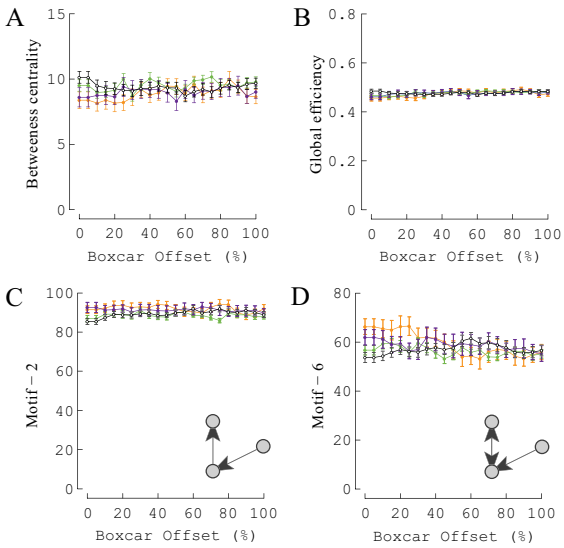

Fig. S4. Network measurements are robust throughout a trial. Betweeness centrality (*A*), global efficiency (*B*), and triadic interaction patterns 2 (*C*) and 4 (*D*) [see *Insets* in graphs and also Sporns and Kotter (1)] were plotted throughout the 30-min trial for *Canton-S* males (n = 43, white), females (n = 26, green), and *Oregon-R* males (n = 28, orange) and females (n = 23, purple). Means plotted here were calculated at 5% increments of the total number of network iterations established throughout the trial and plotted along the x axis. Error bars indicate SEs around the mean. Measurements presented here represent networks at 25% density.

1. Sporns O, Kotter R (2004) Motifs in brain networks. *PLoS Biol* 2:e369.

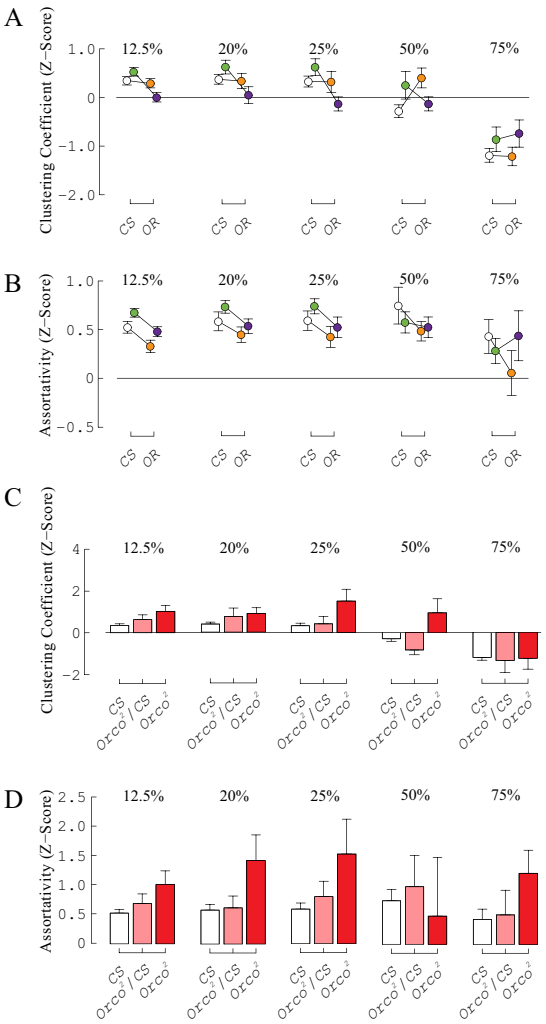

Fig. S5. Trends in assortativity and clustering across a range of densities. Networks were evaluated at 12.5%, 20%, 25%, 50%, and 75% density to determine consistency of network dynamics (see text). *Z* scores were based on 500 simulations, which preserved the in- and out-degree of the iterative networks. (*A* and *B*) Difference between sex and genotypes in clustering coefficient (*A*) displayed a weak, consistent trend for an interaction from 12.5% to 50%, and (*B*) a moderate trend for *Oregon-R* to have a lower assortativity than *Canton-S* from 12.5% to 50% density (*Canton-S* males, n = 43, 43, 43, 42, and 40, white; *Canton-S* females n = 26, 26, 26, 26, and 26, purple; *Oregon-R* males n = 28, 28, 28, 25, and 19, orange; *Oregon-R* females n = 23, 23, 23, 23, and 20, purple, at 12.5%, 20%, 25%, 50%, and 75% density, respectively). (*C* and *D*) Compromising olfaction tended to (*C*) increase the clustering coefficient of $Orco^2$/ $Orco^2$ mutants compared with its controls across a wide range of densities (12.5–50%) and (*D*) increase the assortativity (12.5–25% and 75% density) ($Orco^2$/*Canton-S* n = 27, 25, 24, 21, and 11, light red; $Orco^2$ n = 23, 18, 14, 6, and 2, red, at 12.5%, 20%, 25%, 50%, and 75% density, respectively). Note that the analysis of $Orco^2$ at 75% density is tenuous because the amount of trials that generated at least one network is low (n = 2). Error bars indicate SEs around the mean.

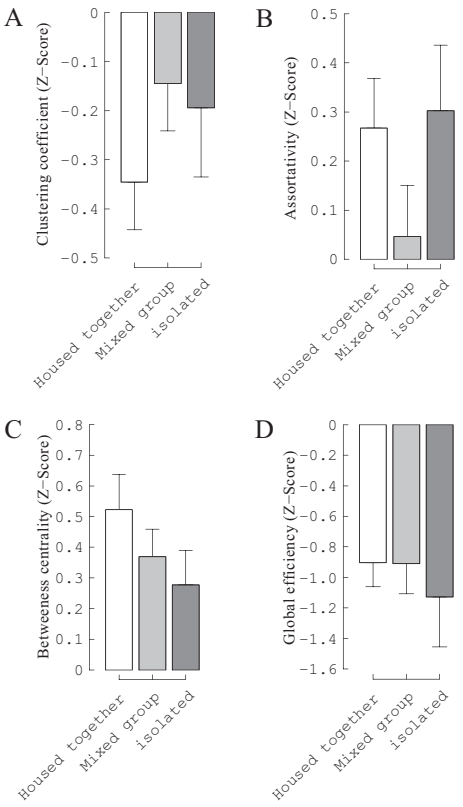

Fig. S6. Adult experience before the experiment has no effect on network dynamics. To examine the effect of experience on social interaction networks, flies housed communally since eclosion (Housed together, $n = 14$) were compared with individuals who had been housed communally in separate groups and then combined (Mixed group, $n = 22$) as well as flies who had been isolated since eclosion (Isolated, $n = 22$). Neither movement, duration of an interaction, rate of interaction, nor interactions reciprocated showed any significant difference ($P = 0.32$, $P = 0.96$, $P = 0.687$, and $P = 0.357$, respectively; not plotted). None of the network measurements tested had any significant effects (*A–D*; clustering coefficient $P = 0.554$, assortativity $P = 0.240$, betweeness centrality $P = 0.318$, or efficiency $P = 0.826$). Error bars indicate SEs around the mean. Networks of 25% density are presented.

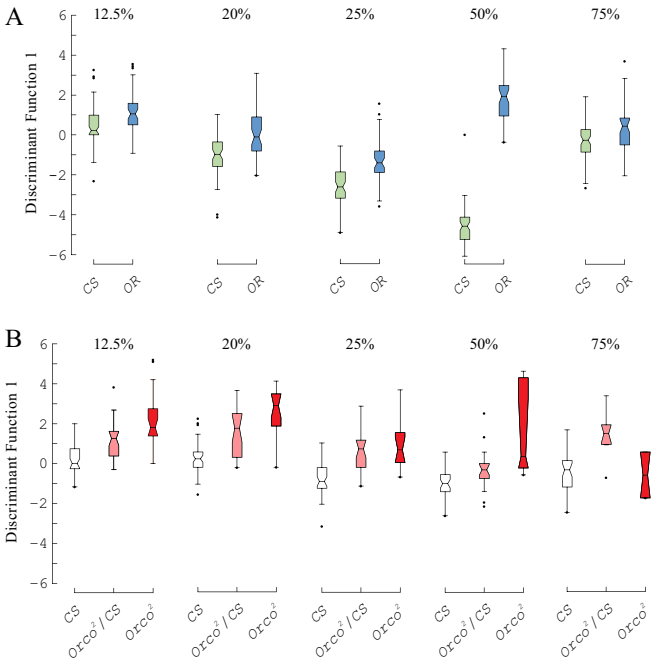

Fig. S7. Discriminant classification based on triadic patterns of interaction. Functional triadic patterns were used (1), and in standardizing these motifs by creating *z* scores, motifs 1 and 3 were necessarily neglected (being solely a function of in- or out-degree, these motifs will always generate a *z* score of 0 when standardizing by in- and out-degree). Discriminant functions were established for each comparison: (*A*) wild-type, and (*B*) *Orco*^{2} for each density level (12.5%, 20%, 25%, 50%, and 75%). (*A*) Wild-type discrimination was poor for 12.5%, 20%, 25%, and 75% (misclassification rate of 42.5%, 41.6%, 31.7%, and 48.6%, respectively) but excellent at 50% (classification rate of 98.2%; *Canton-S* n = 69, 69, 69, 68, and 66, light green; *Oregon-R* n = 51, 51, 51, 48, and 39, light blue, at 12.5%, 20%, 25%, 50%, and 75% density, respectively). (B) Discrimination between *Orco*^{2} and its controls was moderate at densities ranging from 12.5% to 50% (misclassification of control as *Orco*^{2} or *Orco*^{2} as control: 8.6%, 13.9% 18.5%, and 10.1%, at 12.5%, 20%, 25%, and 50% density, respectively; *Canton-S* males, n = 43, 43, 43, and 42, white; *Orco*^{2}/*Canton-S* n = 27, 25, 24, and 21; light red; *Orco*^{2} n = 23, 18, 14, and 6, red, at 12.5%, 20%, 25%, 50%, and 75% density, respectively). The decreased trials successfully networked at higher densities (n = 2 for *Orco*^{2} at 75%) did not allow for evaluation of the discriminating functions at that density. Misclassification was evaluated with a leave-one-out approach. Whiskers on the boxplot represent 1.5 × interquartile range.

1. Sporns O, Kotter R (2004) Motifs in brain networks. *PLoS Biol* 2:e369.

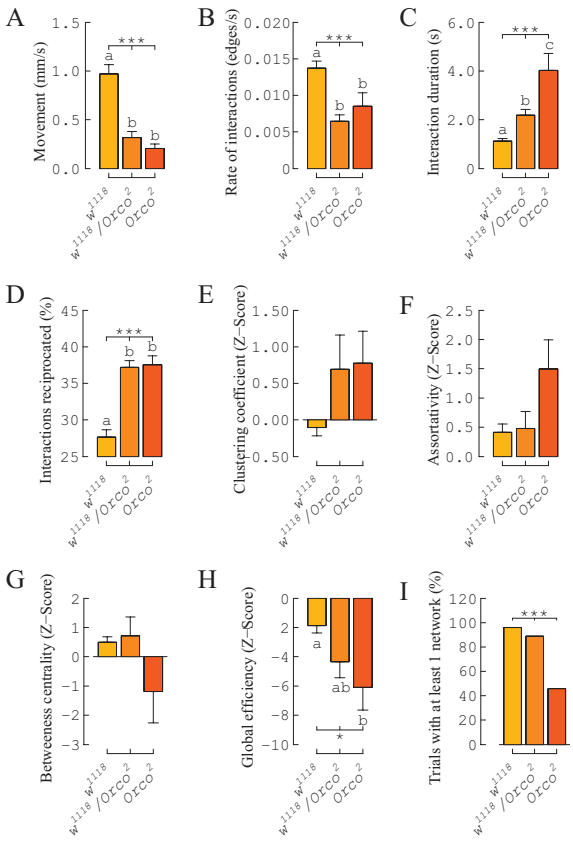

Fig. S8. Olfactory effects on social interaction networks map to the *Orco* locus. The effects of the *Orco* null mutation in a *Canton-S* wild-type strain are shown in Figs. 2 and 3 and Fig. S1. These comparisons are reproduced here for a second genetic background in *A–D*, *E–H*, and *I*, respectively. Only those social interaction network results that were statistically significant for both genetic backgrounds were discussed in the text. Here, the replication of these effects is shown in a w^{1118} background. (*A*) Movement is significantly diminished in homozygous $Orco^2$ and heterozygous $Orco^2/ w^{1118}$ flies compared with the w^{1118} control strain ($P < 0.001$), although this rate of activity differed between strains. (*B*) Rate of interactions is also significantly lower than the control strain in $Orco^2$ and $Orco^2/ w^{1118}$ ($P < 0.001$), consistent with the findings reported for $Orco^2$ in the *Canton-S* genetic background. (*C*) Duration of an interaction is significantly higher in $Orco^2$ compared with the heterozygous $Orco^2/ w^{1118}$, and this in turn is higher than w^{1118} ($P < 0.001$), although this effect is not consistent across backgrounds. (*D*) Percentage of interactions reciprocated is significantly higher in the homozygous $Orco^2$ and heterozygous $Orco^2/ w^{1118}$ compared with the w^{1118} control strain ($P < 0.001$), consistent with the reported effect of homozygous $Orco^2$ in the *Canton-S* genetic background. (*E*) Clustering coefficient is not significantly different between $Orco^2$, heterozygous $Orco^2/ w^{1118}$, and w^{1118} ($P = 0.1327$). (*F*) Assortativity tends to be higher in homozygous $Orco^2$ compared with heterozygous and homozygous controls, although this is not significant after multiple test correction ($P = 0.029$; *Methods*). (*G*) Betweeness centrality is not significantly different between the homozygous $Orco^2$, heterozygous $Orco^2/ w^{1118}$, and homozygous w^{1118} ($P = 0.0947$). (*H*) Global efficiency is significantly lower in homozygous $Orco^2$ compared with homozygous w^{1118} ($P = 0.0123$), consistent with the results of the $Orco^2$ mutation in the *Canton-S* strain. (*I*) Proportion of trials resulting in at least one network is severely reduced in homozygous $Orco^2$ ($P < 0.001$), consistent with the reduced ability of homozygous $Orco^2$ in the *Canton-S* background. Groups are color-coded: w^{1118} ($n = 24$, yellow), $Orco^2/ w^{1118}$ ($n = 21$, light orange), $Orco^2$ ($n = 13$, dark orange). $^*P < 0.05$, $^{**}P < 0.01$, $^{***}P < 0.001$, only when significance is maintained after multiple test corrections. Error bars indicate mean ± 1 SE. Measurements presented here represent networks at 25% density.

Table S1. Classes of interactions displayed while forming a network

Genotype	Front approach (%)	Rear approach (%)	Preening (%)	Misc. (%)	Touch (%)
Canton-S females	27.07	21.83	40.17	10.91	63.31
Canton-S males	23.08	20.94	50.43	5.56	65.81
Oregon-R females	19.93	18.58	47.97	13.51	56.42
Oregon-R males	14.63	14.63	48.08	22.65	44.60
Canton-S (dark)	26.40	28.40	38.80	6.40	75.60
iav^1	17.16	6.93	69.97	5.94	53.80
iav^1/*Canton-S*	26.92	30.77	39.90	2.40	75.97
$Orco^2$	25.17	14.48	46.55	13.79	68.28
$Orco^2$/*Canton-S*	18.26	16.96	53.78	11.30	65.22
$poxn^{\Delta XBs6}$	16.22	9.46	61.15	13.18	51.69
$poxn^{SuperA}$	22.63	20.43	43.43	13.50	57.67

Interactions were categorized according to the behavior of the principal interactor into either: approaching the front (orienting toward the posterior), approaching the rear (orienting toward the anterior), preening (utilization of the fore- or aft legs to repeatedly contact the abdomen, the wings, or the proboscis), or miscellaneous (Misc., not fulfilling the other criteria). Interactions exhibiting more than one type of behavior were classified according to the behavior that occupied the majority of the interaction. The proportion of interactions involving touch included all interactions regardless of category. Observations were tallied over every distinct interaction that occurred within the formation of five networks for each genotype/sex (at 25% density).

Table S2. Probability values for permutation tests: Behavioral measurements

		Measure			
Comparison	Effects	Movement (mm/s)	Rate of interactions (no./s)	Interaction duration (s)	Interactions reciprocated (%)
Canton-S vs. *Oregon-R* males vs. females	Strain	0.1943	**<0.001**	**<0.001**	0.6748
	Sex	0.0472	**<0.001**	**<0.001**	0.7791
	Interaction	0.2173	0.0288	**<0.001**	0.853
Canton-S (♂) vs. *Canton-S* (♂ in the dark)	Vision	0.9785	**<0.001**	**<0.001**	0.2245
Canton-S (♂) vs. iav^1/*Canton-S* (♂) vs. iav^1 (♂)	Audition	0.1082	**<0.001**	0.1315	**0.0107**
Canton-S (♂) vs. $Orco^2$/*Canton-S* (♂) vs. $Orco^2$ (♂)	Olfaction	**0.0197**	**<0.001**	0.4872	**<0.001**
w^{1118} (♂) vs. (w^{1118})$Orco^2$/w^{1118} (♂) vs. (w^{1118})$Orco^2$ (♂)	Olfaction	**<0.001**	**<0.001**	**<0.001**	**<0.001**

Each comparison was evaluated by comparing the empirical *F* statistic against a distribution created by permutation. *P* values significant after multiple test correction (*false discovery rate*) are indicated in bold (see main text and *SI Methods*). For $Orco^2$, although interaction duration is significant in a w^{1118} background, it is not significant in a *Canton-S* background and was therefore not reported.

Table S3. Probability values for permutation tests: Social interaction network measurements

		Measure			
Comparison	Effects	Clustering coefficient (*Z* scores)	Assortativity (*Z* scores)	Betweenness centrality (*Z* scores)	Global efficiency (*Z* scores)
Canton-S vs. *Oregon-R* males vs. females	Strain	0.0191	0.0738	**0.0121**	0.6792
	Sex	0.6384	0.2576	0.5449	0.7488
	Interaction	0.0231	0.8205	0.7654	0.4228
Canton-S (♂) vs. *Canton-S* (♂ in the dark)	Vision	0.0363	0.4961	0.0332	0.0988
Canton-S (♂) vs. iav^1/*Canton-S* (♂) vs. iav^1 (♂)	Audition	0.2925	0.4254	0.2966	0.2995
Canton-S (♂) vs. $Orco^2$/*Canton-S* (♂) vs. $Orco^2$ (♂)	Olfaction	0.0192	0.0475	0.6485	**0.0054**
w^{1118} (♂) vs. (w^{1118})$Orco^2$/w^{1118} (♂) vs. (w^{1118})$Orco^2$ (♂)	Olfaction	0.1327	0.029	0.0947	**0.0123**

Each comparison was evaluated by comparing the empirical *F* statistic against a distribution created by permutation. *P* values significant after multiple test correction (*false discovery rate*) are indicated in bold (see main text and *SI Methods*).

Movie S1. High-definition examples of interactions between *Drosophila melanogaster*. Analysis of slow-motion movies demonstrates leg contact across three broad interaction classes: approach from the front, approach from the rear, and preening (followed by an approach from the rear). Acquired at 500 fps with a PCO Dimax camera and a Tamron SP AF90-mm F2.8 lens.

Movie S1

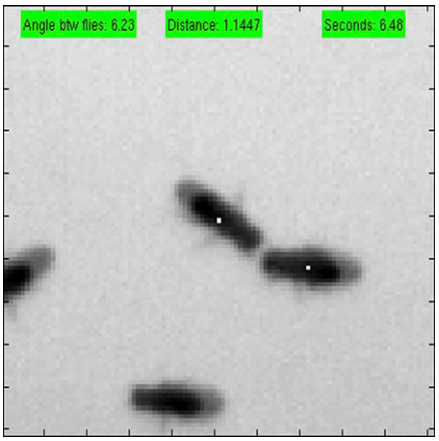

Movie S2. Interactions flagged by our classifier (Fig. 1*A*) that were subsequently determined to be frontal approaches. The angle and distance between the principal interactor (digitally dotted, centered fly) and interactee (digitally dotted) is indicated, as well as the time (in seconds) of the interaction (highlighted in green when they satisfy our criteria). If the principal interactor is interacting (according to our criteria), it is dotted white. Similarly, if the interactee (in this frame of reference) is interacting with the centered fly, it is dotted white; when a fly is not interacting, it is dotted black. Acquired at 25 fps with a Point Gray FireflyMV and a 6-mm μ-lens.

Movie S2

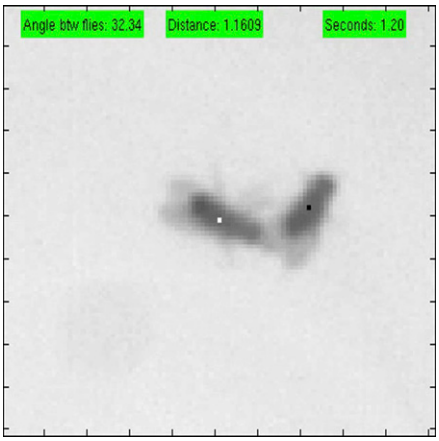

Movie S3. Interactions flagged by our classifier (Fig. 1*A*) that were subsequently determined to be rear approaches. The angle and distance between the principal interactor (digitally dotted, centered fly) and interactee (digitally dotted) is indicated, as well as the time (in seconds) of the interaction (highlighted in green when they satisfy our criteria). If the principal interactor is interacting (according to our criteria), it is dotted white; similarly, if the interactee (in this frame of reference) is interacting with the centered fly, it is dotted white; when a fly is not interacting, it is dotted black. Acquired at 25 fps with a Point Gray FireflyMV and a 6-mm μ-lens.

Movie S3

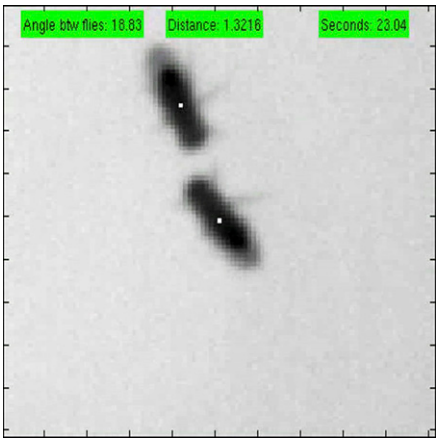

Movie S4. Interactions flagged by our classifier (Fig. 1*A*) that were subsequently determined to involve large amounts of preening. The angle and distance between the principal interactor (digitally dotted, centered fly) and interactee (digitally dotted) is indicated, as well as the time (in seconds) of the interaction (highlighted in green when they satisfy our criteria). If the principal interactor is interacting (according to our criteria), it is dotted white; similarly, if the interactee (in this frame of reference) is interacting with the centered fly, it is dotted white; when a fly is not interacting, it is dotted black. Acquired at 25 fps with a Point Gray FireflyMV and a 6-mm μ-lens.

Movie S4

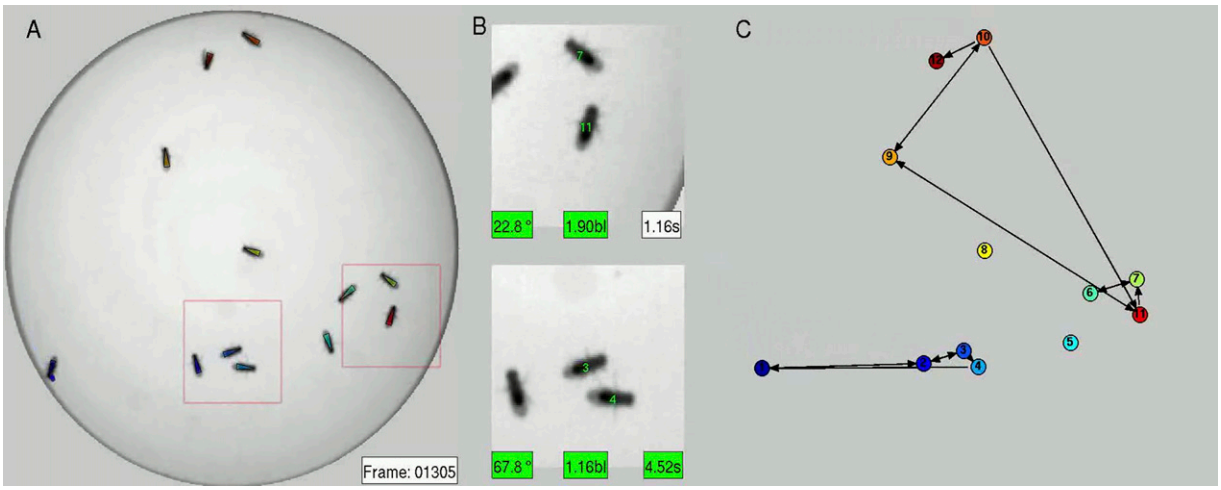

Movie S5. An example of network formation in wild-type *Drosophila melanogaster*. (*A*) Video sequence overlaid with triangles indicating the position and orientation of the flies (as determined by Ctrax). Interactions are highlighted with a semiopaque red box around any flies currently in an interaction (according to our criteria; Fig. 1*A*). (*B*) Close-up view of interactions currently satisfying our criteria. The angle and distance between the principal interactor (numbered and centered fly) and interactee (numbered) is indicated, as well as the time (in seconds) of the interaction (highlighted in green when they satisfy our criteria). (*C*) A running tally of interaction history is recorded and plotted between the current positions (as determined by Ctrax), illustrating the time-invariance of interaction history accumulation leading to network formation. The end sequence of the movie rearranges the network (from position of the flies to a force-directed network layout).

Movie S5